



Published in final edited form as:

J Alzheimers Dis. 2018 ; 65(4): 1301–1312. doi:10.3233/JAD-180570.

Atrophy in Distributed Networks Predicts Cognition in Alzheimer's Disease and Type 2 Diabetes

Stephanie S. Buss^a, Jaya Padmanabhan^a, Sadhvi Saxena^{a,b}, Alvaro Pascual-Leone^{a,c}, Peter J. Fried^{a,*}

^aBerenson-Allen Center for Noninvasive Brain Stimulation, Division of Cognitive Neurology, Department of Neurology, Beth Israel Deaconess Medical Center, Harvard Medical School, Boston, MA, USA

^bDepartment of Neurology, Johns Hopkins University School of Medicine, Baltimore, MD, USA

^cInstitut Guttmann, Universitat Autònoma de Barcelona, Badalona, Barcelona, Spain

Abstract

Background: Alzheimer's disease (AD) and type 2 diabetes (T2DM) are common causes of cognitive decline among older adults and share strong epidemiological links. Distinct patterns of cortical atrophy are observed in AD and T2DM, but robust comparisons between structure-function relationships across these two disease states are lacking.

Objective: To compare how atrophy within distributed brain networks is related to cognition across the spectrum of cognitive aging.

Methods: The relationship between structural MRI changes and cognition was studied in 22 mild-to-moderate AD, 28 T2DM, and 27 healthy participants. Cortical thickness measurements were obtained from networks of interest (NOIs) matching the limbic, default, and frontoparietal resting-state networks. Composite cognitive scores capturing domains of global cognition, memory, and executive function were created. Associations between cognitive scores and the NOIs were assessed using linear regression, with age as a covariate. Within-network General Linear Model (GLM) analysis was run in Freesurfer 6.0 to visualize differences in patterns of cortical atrophy related to cognitive function in each group. A secondary analysis examined hemispheric differences in each group.

Results: Across all groups, cortical atrophy within the limbic NOI was significantly correlated with Global Cognition ($p = 0.009$) and Memory Composite ($p = 0.002$). Within-network GLM analysis and hemispheric analysis revealed qualitatively different patterns of atrophy contributing to cognitive dysfunction between AD and T2DM.

*Correspondence to: Dr. Peter Fried, Berenson-Allen Center for Noninvasive Brain Stimulation, Beth Israel Deaconess Medical Center, 330 Brookline Ave (KS 158), Boston, MA, 02215, USA. Tel.: +1 617 667 0224; Fax: +1 617 975 5322; pfried@bidmc.harvard.edu.

SUPPLEMENTARY MATERIAL

The supplementary material is available in the electronic version of this article: <http://dx.doi.org/10.3233/JAD-180570>.

Conclusion: Brain network atrophy is related to cognitive function across AD, T2DM, and healthy participants. Differences in cortical atrophy patterns were seen between AD and T2DM, highlighting neuropathological differences.

Keywords

Alzheimer's disease; cognitive aging; dementia; diabetes mellitus; executive function; memory disorders

INTRODUCTION

The number of people aged 65 and older is expected to reach one billion worldwide by 2030 [1, 2]. Aging is the strongest risk factor for neurodegenerative disease including Alzheimer's disease (AD). Atrophy patterns are closely tied to cognitive function in dementia [3], and probing these structure-function relationships in AD has diagnostic, prognostic, and interventional utility [4-6]. Neuroimaging studies in AD have shown a characteristic pattern of cortical thinning associated with disease severity [7]: impairments in learning tend to be associated with greater atrophy of the temporal pole, while hippocampal and medial temporal lobe atrophy are more predictive of impairments with delayed recall and recognition [8]. In patients with mild cognitive impairment (MCI), cortical atrophy measures can predict risk of progression to AD-type of dementia, with cortical thickness as the strongest individual prognostic marker [9].

Structure-function relationships in other forms of pathological aging are less thoroughly characterized. In older adults, type 2 diabetes (T2DM) has been associated with declines in processing speed, attention, executive function, and free memory recall [10]. Older adults with T2DM show global atrophy and increased burden of microvascular disease [11, 12]. Brain atrophy in T2DM is correlated with disease severity and duration, and may reflect additional neurodegenerative mechanisms aside from microvascular disease [12, 13]. While T2DM is often associated with vascular dementia (VaD), it is also linked to an almost twofold increased risk of AD, likely reflecting a complex interplay between vascular, neurodegenerative, and neurotoxic factors [14]. In order to identify neuroimaging targets for future intervention in T2DM, and determine which patients are at highest risk of cognitive decline, it would be useful to know whether T2DM exhibits similar structure-function relationships to AD. However, prior studies of cortical atrophy and cognition in AD and T2DM have focused on single disease states, examined separate disease-specific regions of interest, or used atrophy measures other than cortical thickness [15, 16], limiting generalizability.

Measuring cortical thickness within functionally connected brain networks of interest (NOIs) represents a middle-ground between whole-brain analysis and localized region-of-interest methods, offering a potentially powerful tool to quantify atrophy within distributed brain networks. Resting state functional connectivity MRI (rs-fcMRI) can be used to parcelate the brain into functionally connected but spatially separate brain regions showing correlated activity [17]. Recent studies have suggest that these intrinsic brain networks play a role in the distribution, and possibly the pathogenesis, of proteins involved in

neurodegenerative diseases [18]. In AD, patterns of tau deposition follow functionally connected brain networks, and greater pathology within these tau-networks is related to disease progression on Braak staging [19]. Prior studies have used an NOI approach to compare cortical atrophy, amyloid- β ($A\beta$) deposition, and tau distribution in AD [20]. The present study extends the NOI approach one step further, using NOIs to compare the relationship between cortical atrophy and cognition across the spectrum of cognitive aging.

This study used a network-based approach to analyze structure-function relationships between cortical thickness and cognitive function in T2DM and AD participants aged 50 and older, compared to healthy, cognitively-intact older adults. The study tested the hypothesis that declines in global cognition, memory, and executive function would be associated with atrophy in distributed brain NOIs across different conditions of cognitive aging. Furthermore, the study tested the hypothesis that the pattern of atrophy and its relationship to cognitive function would vary between T2DM and AD participants, reflecting differences in underlying brain pathology.

MATERIALS AND METHODS

Participants

Neuroimaging and neuropsychological data from 77 adult study participants aged 50 and older who participated in research from 2011 to 2015 at the Berenson-Allen Center for Noninvasive Brain Stimulation at Beth Israel Deaconess Medical Center (BIDMC) were included in this retrospective cross-sectional study. The study was approved by the BIDMC Institutional Review Board, and all study participants provided written informed consent upon enrollment consistent with the Declaration of Helsinki. Study participants comprised three groups: 22 AD, 28 T2DM, and 27 healthy controls (HC). Inclusion criteria in the AD group were a clinical diagnosis of probable mild-to-moderate AD according to DSM-V/NINCDS-ADRDA criteria [21], a Clinical Dementia Rating Scale (CDR) of 1, and a Mini-Mental Status Examination (MMSE) ranging from 18–24. Inclusion criteria for the T2DM participants included a clinical diagnosis of T2DM, relatively good glucose control with an A1c $\leq 10\%$, and normal cognition (MMSE ≥ 27). HC participants were required to have normal cognition (MMSE ≥ 27) and be non-diabetic (A1c < 6.2). All participants underwent equivalent testing, including a standardized neurological exam, medical history review, formal neuropsychological testing, and a structural MRI scan. Participants were excluded if they had unstable medical conditions, neuropsychiatric conditions, or premorbid IQ below 80 as measured by the age-adjusted Wechsler Test of Adult Reading (W-TAR).

Neuropsychological testing

Neuropsychological memory testing was performed by a trained psychometrist. Testing included the MMSE and Geriatric Depression Scale (GDS; 15-item) drawn from the National Alzheimer's Coordination Center's Uniform Data Set version 1.1 [22]. The Trail Making Test (TMT) was administered, and the time difference in seconds that it took each subject to complete TMT B versus TMT A was calculated (TMT_{B-A}). The Digit Symbol Substitution Test (DSST; number correct in 90 seconds), Digit Span Backwards Length (DSB Length; longest digit span), Logical Memory Story (LMS) Story-A were drawn from

the Wechsler Memory Scale-Revised. The LMS included an immediate story recall score (LMS Immediate Recall) and a delayed 30-minute recall score (LMS Delayed Recall) without cueing. Additionally, the Alzheimer's Disease Assessment Scale-Cognitive Subscale was administered, and the total score (ADAS-Cog Total; 70 item), word list immediate recall subscore (ADAS-Cog Immediate Recall), and word list delayed recognition subscore (ADAS-Cog Delayed Recognition) were analyzed independently [23]. The Rey Auditory Verbal Learning Test (RAVLT) was also administered, and sub-scores of percent correct responses analyzed included a percent correct during initial learning (RAVLT Immediate Recall), 20 minute delayed recall (RAVLT Delayed Recall), and delayed recognition (RAVLT Delayed Recognition) [24, 25]. Neuropsychological scores were not obtained for ADAS-Cog Recall and ADAS-Cog Recognition in one AD participant and one HC, for RAVLT Delayed Recognition in one T2DM participant, for the DSST in one AD participant, and for TMT_{B-A} in one T2DM participant and six AD participants (four of whom were unable to complete either TMT A or TMT B). These participants were excluded from analysis of those missing measures alone.

For each neuropsychological measure, z-scores were calculated by subtracting each individual score from the mean score of the all three groups and dividing by the standard deviation across all three groups. Scores of the TMT_{B-A}, ADAS-Cog Total, ADAS-Cog Immediate Recall, and ADAS-Cog Delayed Recognition were inverted so that higher scores reflected better performance across all tests. Following an approach from the Alzheimer's Disease Neuroimaging Initiative, composite scores were computed by averaging together z-scores from individual tests so that atrophy patterns could be related to cognitive domains more generally [26, 27]. A Memory Composite was created by from the RAVLT Immediate Recall, RAVLT Delayed Recall, RAVLT Delayed Recognition, LMS Immediate Recall, LMS Delayed Recall, ADAS-Cog Recall, and ADAS-Cog Recognition. An Executive Composite was computed by averaging the z-scores of DSB Length, TMT_{B-A}, and DSST. Global Cognition was measured using the ADAS-Cog Total, which is already a composite score of multiple subtests.

MRI imaging data

A T1-weighted anatomical magnetic resonance imaging scan was obtained in all participants on a 3T scanner (GE Healthcare, Ltd., UK) using a 3D spoiled gradient echo sequence: 162 axial-oriented slices for whole-brain coverage; 240-mm isotropic field-of-view; 0.937-mm × 0.937-mm × 1-mm native resolution; flip angle = 15°; TE/TR 2.9/6.9 ms; duration 432 s. T1-weighted anatomical MRIs were analyzed with Freesurfer 6.0 (documented and freely available online at <http://surfer.nmr.mgh.harvard.edu/>). The technical details of these procedures are described in prior publications [28-41]. To ensure overall accuracy of segmentations and parcellations, all reconstructions were subjected to a rigorous data quality control process: a trained rater reviewed and manually corrected reconstructions when necessary, which were reviewed by an independent rater.

In addition to thickness of neocortical areas, hippocampal volume was calculated in Freesurfer and corrected for individual head size by dividing by total intracranial volume. One T2DM participant with an intracranial volume greater than two standard deviations

above the mean was excluded from this analysis alone. Normed hippocampal volumes were then converted to z-scores over all three groups (following the same procedure as the neuropsychological scores) in order to compare hippocampal atrophy between groups.

Measures of network atrophy

Atrophy across distributed brain networks, referred to herein as “network atrophy,” was defined using gray matter cortical thickness measurements within predefined NOIs. NOIs were derived from a 1000-subject group average rs-fcMRI analysis from Yeo and colleagues [17]. Cortical thickness was selected as the primary measure of atrophy because it is robust to head size and gender bias [42], and shows promise as a marker of disease progression and conversion from MCI to AD [9]. A previous study in AD used an equivalent rs-fcMRI parcellation approach to compare cortical atrophy, neurodegenerative protein deposition, and brain metabolism across cortical NOIs, but did not examine associations with cognition [20]. Another study in healthy adults found a relationship between NOI-based cortical thickness and executive function, but used a different technique to define NOIs, and did not examine memory function [43]. To our knowledge, this technique has not been previously used to make structure-function comparisons across different disease states.

NOIs were selected to encompass the limbic, default, and frontoparietal networks as defined by group-level functional connectivity maps from Yeo and colleagues [17] (Supplementary Figure 1). The limbic and default networks were chosen because these networks encompass brain regions with high levels of neuropathology on Braak staging [44], and include the entorhinal cortex, parahippocampal gyrus, and temporal pole which are implicated in memory encoding and retrieval [45-49]. The frontoparietal network was chosen because it shows high A β distribution and hypometabolism in AD [20], and is thought to play an important role in executive function [43, 50, 51]. Average cortical thickness (in mm) was assessed within each NOI bilaterally. Given the potential for functional specialization and hemispheric asymmetrical atrophy patterns, the left and right hemispheres of each NOI were also measured for use in a secondary analysis.

Statistical analysis

Statistical analyses were performed using JMP Pro 13.0 (SAS Institute Inc., Cary, NC) and Stata 14.2 (StataCorp, College Station, TX). Significance was determined with a two-tailed 95% confidence interval ($\alpha = 0.05$). Baseline characteristics were compared for group differences. In the primary analysis, linear regression was used to determine the relationship between cortical thickness and cognitive measures across all three groups. To visualize the within-network atrophy patterns in each group contributing to structure-function relationships, a General Linear Model (GLM) analysis was run using Freesurfer 6.0. Finally, a secondary hemispheric analysis was performed using linear regression to test if there was right/left asymmetry contributing to the relationship between network atrophy and cognition.

Baseline characteristics

Demographics and cognitive scores from some T2DM and HC participants have been previously reported [52]. Baseline characteristics including demographics, atrophy

measures, and z-scored neuropsychological measures were tested for significant differences across all three groups. Fischer's exact test was used for dichotomous variables, and oneway analysis of variance (ANOVA) was used for continuous variables. Tukey's Honestly Significant Difference (HSD) was used for *post hoc* comparisons between each group. Since *age* was different between the groups (see Results), and was expected to relate to both brain atrophy and cognition, it was added as a covariate to all subsequent analyses.

To ensure that our dataset was consistent with prior literature [53], the relationship between right and left hippocampal volumes and RAVLT Delayed Recognition were tested in separate linear regression analyses for each group, with *age* as a covariate. For hippocampal volume analysis, uncorrected *p*-values are reported, and significance is indicated after correction using the Benjamini-Hochberg procedure for controlling the False Discovery Rate (FDR) with a global $\alpha = 0.05$ [54].

Linear regression

Multiple linear regression analyses were preformed to assess the relationship between cognitive function and network atrophy (with each NOI separately to avoid collinearity) as well as the influence of participant *age* and *diagnosis*. Global Cognition, Memory Composite, and Executive Composite scores were entered as dependent variables into a fixed-effects linear model with the main independent factors of *diagnosis* (AD, T2DM, HC), *thickness*, the *diagnosis*thickness* interaction term, and *age* as a covariate. Uncorrected *p*-values are reported, and significance is indicated after correction using the Benjamini-Hochberg procedure for FDR with a global $\alpha = 0.05$ [54].

GLM analysis

A GLM analysis using a familywise error rate of 0.05 was run in Freesurfer 6.0 for each neuropsychological test associated with a NOI atrophy in the AD and T2DM groups. GLM analysis was restricted to vertices within the relevant NOI to identify regions within the network that were significantly associated with that neuropsychological measure, with *age* as a covariate.

Hemispheric analysis

Separate linear regression analyses were preformed using cortical thicknesses within right and left hemisphere NOIs. Linear regression was used to test the associations of memory tests with NOI thickness and hippocampal volumes, with *age* as a covariate. Only uncorrected *p*-values are reported in the secondary analysis.

RESULTS

Baseline characteristics

AD participants were significantly older than the HC group, and reported higher depression scores on the GDS (Table 1). The AD group showed atrophy within all NOIs and reduced hippocampal volume compared to HC and T2DM. No significant differences in network thickness or corrected hippocampal volume were seen between T2DM and HC groups. AD

participants scored significantly worse on all cognitive tests compared to HC, and T2DM group scored in the intermediate range between the AD and HC on multiple measures.

Left hippocampal volume was associated with RAVLT Delayed Recognition in AD ($p = 0.0029$) and T2DM ($p = 0.019$). After correction with FDR, only the association in AD remained significant.

Multiple linear regression

None of the analyses yielded a significant *diagnosis*thickness* interaction (p values > 0.09), indicating no effect modification. Therefore, the models were rerun without the interaction term. Linear regression relationships between cortical thickness and composite cognitive scores are shown in Fig. 1.

Limbic NOI

There was a significant main effect of cortical thickness in the linear models for Global Cognition ($p = 0.009$) and Memory Composite ($p = 0.002$), indicating that limbic network atrophy was related to global cognition and memory function independent of group and controlling for *age*. After adjusting for multiple comparisons with FDR, both relationships remained significant.

Default NOI

There were no significant associations between cortical thickness within the default NOI and Global Cognition, Memory Composite, or Executive Composite.

Frontoparietal NOI

For Executive Composite, the linear model showed a main effect of cortical thickness ($p = 0.033$), indicating that frontoparietal network atrophy was related to memory function independent of group and controlling for *age*. This relationship was not significant after adjusting for multiple comparisons using FDR.

GLM analysis

Within-network GLM analysis relating cortical thickness in the limbic NOI with cognitive scores are shown for Global Cognition (Supplementary Figure 2) and Memory Composite (Supplementary Figure 3). In the AD group, cortical thickness within the medial temporal lobes was associated with Global Cognition and Memory Composite, with a left hemisphere predominance. In T2DM, cortical thickness in the anterior temporal, inferior temporal, and orbitofrontal cortex showed associations with both Global Cognition and Memory Composite. Supplementary Figure 4 shows associations between cortical thickness within the frontoparietal NOI and Executive Composite. In AD, cortical thickness in the superior frontal, parietal, and posterior temporal cortex was associated with Executive Composite. In T2DM, associations between cortical thickness and Executive composite were driven by anterior regions of the frontoparietal NOI, including regions of the left dorsolateral prefrontal cortex.

Secondary hemispheric analysis

Supplementary Figure 5 shows associations between right and left NOI thickness measures and neuropsychological tests in each group. Given the exploratory nature of these analyses, *p*-values for the supplementary hemispheric analysis were not corrected for multiple comparisons and should be interpreted accordingly. Measures of global decline in AD were associated with atrophy in both the left limbic network and left default network. Structure-function relationships between limbic NOI thickness and memory tests showed a strong left hemisphere predominance. Furthermore, there was a double dissociation between cortical thickness and cognition, with limbic network atrophy associated with memory function and frontoparietal network atrophy associated with executive function, which was seen only in the AD group. In T2DM thickness within the default NOI showed associations with both Memory Composite and Executive Composite. In HC, atrophy within all three networks was associated with RAVLT Delayed Recall.

DISCUSSION

The present study employed a relatively novel network-based approach to examine structure-function relationships impacting cognition across the spectrum from healthy to pathological cognitive aging. The primary hypothesis, that atrophy within distributed brain networks would be associated with declines in cognition across AD, T2DM, and HC, was upheld. Qualitative differences in structure-function relationships within AD and T2DM were observed following exploratory within-network GLM and hemispheric analyses. This suggests that different patterns of atrophy drive structure-function relationships in T2DM and AD, reflecting separable neurobiological substrates across different forms of pathological aging. Understanding these differences may help target future therapies aimed at slowing cognitive decline.

The limbic network contains anterior medial temporal regions including the entorhinal cortex, implicated in memory consolidation and retrieval, as well as the temporal pole, which is important in semantic memory encoding. In structural MRI studies in AD, gray matter atrophy is greatest in regions that comprise the limbic network, followed by those in the default network regions, with relative sparing of the frontoparietal network regions [20]. Additionally, regions within the limbic network experiences significant hypometabolism as shown with FDG-PET, but have relatively lower A β plaque burden compared to other networks [20]. The present study adds to existing literature by correlating limbic network atrophy with global cognitive and memory function across AD, T2DM, and HC. Left lateralization of these relationships in AD may be related to the semantic demands of verbal learning tests. The study also replicated the previously well-described association between medial temporal atrophy and recognition memory in AD [8, 55]. The limbic network's structural relevance is supported by both seed-based fMRI methods and white matter tractography studies [56, 57]. Sub-regions of the temporal pole are involved in separable large-scale brain networks, suggesting that this area represent a multimodal "hub" integrating sensory, language, and limbic information [56]. The present finding of strong structure-function relationships within the limbic network suggests that breakdown in multimodal "hubs" may play a key role in cognitive decline for AD and as well as other

forms of cognitive aging. However, direct comparisons with rs-fcMRI literature are limited due to concerns that the orbitofrontal and temporal pole are highly prone to artefactual signal on rs-fcMRI [58]. Findings from the present study, which implicate the limbic network, should be interpreted with the caveat that the exact boundaries of this network may show modality-specific variations.

The default network is intrinsically present in the absence of externally-oriented cognitive activity, and deactivated by tasks requiring sustained attention [59]. Impairments in default network connectivity are thought to develop early in AD pathology, and can be seen even in asymptomatic individuals at high risk of AD, including patients with autosomal dominant AD mutations or in healthy older adults with A β deposition [60, 61]. In T2DM, aberrant functional connectivity in the default network is associated with both declines in executive function on a verbal fluency test and with increased insulin resistance [62]. Findings from the present study found no significant associations between default network atrophy and cognition. This contrasts with rs-fcMRI literature showing impairment in functional connectivity within the default network in both AD and T2DM [63, 64], and suggests a dissociation between functional and structural neuroimaging biomarkers. One hypothesis is that, while abnormal connectivity and atrophy within the default network may play an important role in cognitive decline during the preclinical AD, limbic and frontoparietal network atrophy may drive structure-function relationships during later disease stages when atrophy and cognitive decline are more advanced.

The frontoparietal network is implicated in tasks requiring complex attentional control in healthy older adults [43, 51]. In AD, the frontoparietal network shows high A β deposition and FDG-PET hypometabolism, but less atrophy compared to the limbic and default networks [20]. AD also shows increased functional connectivity in frontally-connected distributed networks, with the amount of increase related to executive function performance [65]. One possibility is that increased functional connectivity in the frontoparietal network in AD may be related to a compensatory strategy in the presence of default network dysfunction [66]. The present study adds the finding that atrophy frontoparietal network was significantly associated with executive function in both AD and T2DM. Overall, the structure-function relationship within the frontoparietal network suggests that network-based cortical atrophy and resting-state functional connectivity may have separable effects on cognition, and should be examined independently.

In the primary model, there was no significant *diagnosis*thickness* interaction. Thus, overall structure-function relationships were not significantly different between the groups, despite the significantly greater amount of atrophy in AD compared to HC and T2DM. With the caveat that the present study may not have had sufficient power to detect more subtle differences, this finding nonetheless supports the idea that examining network atrophy may be a useful tool for comparing structure-function relationships among different patient populations. Additionally, within-network GLM and hemispheric analyses did reveal qualitative differences in the atrophy pattern driving the associations among the three groups. These group-specific differences in atrophy patterns likely reflect different underlying neuropathological processes in different disease states.

The mechanisms of neurotoxicity in T2DM and AD are complex and overlapping, and individual patients often present with more than one pathology. In animal models of AD, elements of the neurodegenerative cascade include oligomeric A β [67], tau [44], APOE [68], lipid metabolism [69, 70], and altered synaptic plasticity [71, 72]. Insulin resistance is an additional mechanism that is common to both T2DM and AD. Impaired insulin signaling may have multiple downstream effects including alterations in glucose metabolism, increased tau accumulation, and oxidative stress [73]. In a prospective study of non-demented adults, insulin resistance at baseline predicted subsequent atrophy of the hippocampus and parahippocampal gyrus and impaired performance on RAVLT encoding trials [13]. In healthy adults, hyperglycemia is associated with cortical thinning in AD-associated regions including the parahippocampal gyrus and temporal pole [74]. Furthermore, in observational studies, T2DM almost doubled the risk of developing AD [75]. Even in non-diabetic AD patients, there is impaired insulin and IGF-1 sensitivity in the hippocampus, and reduced insulin responses are associated with impaired episodic memory [76]. The present study adds the finding that cortical atrophy patterns drive structure-function relationships in both T2DM and AD, and that the effect is not significantly different by group. Qualitative differences seen on GLM and secondary analysis in each group are likely to be the product of separable degenerative processes, which converge to cause atrophy in distributed brain networks. Comparing brain structure-function relationships in T2DM and AD can highlight neurotoxic mechanisms leading to the increased risk of dementia in T2DM, improving prognostication in patients at risk of AD [77]. Since insulin resistance is amenable to multiple medication and lifestyle medications, it represents a promising therapeutic target to promote healthy cognitive aging [78].

Understanding the structure-function relationships that are most relevant in different forms of pathological aging may help target future therapies aimed at slowing cognitive decline. Since many older adults have more than one comorbid pathology affecting cognition, any effective treatment targeting pathological aging will require a high degree of individualization. Knowledge of network-based structure-function relationships can facilitate development of investigational therapies aimed at slowing cognitive decline and prevention onset of dementia, including both lifestyle and neuromodulatory approaches. For example, in our hemispheric analysis, the LMS Immediate Recall test was impaired in both T2DM and AD, and was associated with NOI atrophy, yet the association was driven by distinct networks and showed different hemispheric lateralization. In the future, this knowledge could be applied to an individual patient's structural imaging and cognitive profile, and used to target network-based therapies such as non-invasive brain stimulation (NBS). Neuromodulatory treatments are currently being investigated in AD [79, 80]. However, it is not yet known which brain regions or cognitive functions would be most useful to target in patients with other forms of pathological aging. Additionally, it is possible that combining NBS with interventions aimed at reducing insulin resistance such as diet and exercise might be more effective in treating certain populations, including AD patients with concurrent T2DM or pre-diabetes. These questions require further systemic study.

Strengths of this study include a well-characterized study population with in-depth neuropsychological testing and neuroimaging among three groups on a spectrum of cognitive aging. This study was the first of its kind to use a network-based approach to make

inferences about structure-function relationships among different forms of pathological aging. Our method demonstrated differences in patterns of network atrophy associated with cognitive decline in AD and T2DM, despite different severity of cortical atrophy and cognitive deficits in each group.

There are factors which may limit the generalizability of our findings. Our study had a relatively small sample size in each group, which limited the power of our secondary analyses. Our hemispheric analysis did not replicate structure-function relationships in HC seen in other studies, which had larger numbers of participants [43, 50]. Follow up studies in larger datasets would be required to confirm the hemispheric differences, and further elucidate patterns of atrophy that are driving structure-function relationships on GLM. Additionally, there was limited information about diabetes status in the AD cohort, and our T2DM and HC cohorts did not have CSF or PET A β biomarkers to rule out pre-symptomatic AD. However, since any overlap in pathology would have been expected to make group differences less robust, we do not think this significantly impacted the validity of our findings.

Conclusion

Prior research has found strong correlations between network atrophy and cognitive decline in AD [7, 8], but lacks a direct comparisons of patterns of structure-function relationships across a spectrum of cognitive aging. The present study demonstrates that atrophy within global brain networks is related to severity of overall cognitive dysfunction across AD, T2DM, and HC. Qualitative differences in the pattern of atrophy were seen in AD and T2DM, highlighting differences in neuropathologic mechanisms. In the future, measuring structure-function relationships may improve prognostication for older adults at high risk of cognitive decline [77], and allow for individualized targeting of future therapies using pharmacologic, lifestyle-based, and neuromodulatory approaches to promote healthy cognitive aging.

Supplementary Material

Refer to Web version on PubMed Central for supplementary material.

ACKNOWLEDGMENTS

This study was primarily supported by grants from the National Institutes of Health (NIH; R21 NS082870, R21 AG051846). S.S.B. was further supported by the Sidney R. Baer Jr. Foundation (01028951) and the American Academy of Neurology (2016-0229). A.P.L. was also supported by the Sidney R. Baer, Jr. Foundation, Harvard Catalyst | The Harvard Clinical and Translational Science Center (NCRR and the NCATS NIH, UL1 RR025758), the Football Players Health Study at Harvard University, and by the Defense Advanced Research Projects Agency (DARPA) via HR001117S0030. The content is solely the responsibility of the authors and does not necessarily represent the official views of Harvard Catalyst, Harvard University and its affiliated academic health care centers, the National Institutes of Health, the American Academy of Neurology, the Sidney R. Baer Jr. Foundation, The Football Platers Health Study, or DARPA.

Authors' disclosures available online (<https://www.j-alz.com/manuscript-disclosures/18-0570r1>).

REFERENCES

- [1]. Christensen K, Doblhammer G, Rau R, Vaupel JW (2009) Ageing populations: The challenges ahead. *Lancet* 374, 1196–1208. [PubMed: 19801098]
- [2]. National Institute on Aging (2007) Why Population Aging Matters: A Global Perspective. <https://www.nia.nih.gov/sites/default/files/2017-06/WPAM.pdf>
- [3]. Jack CR, Knopman DS, Jagust WJ, Petersen RC, Weiner MW, Aisen PS, Shaw LM, Vemuri P, Wiste HJ, Weigand SD, Lesnick TG, Pankratz VS, Donohue MC, Trojanowski JQ (2013) Tracking pathophysiological processes in Alzheimer's disease: An updated hypothetical model of dynamic biomarkers. *Lancet Neurol* 12, 207–216. [PubMed: 23332364]
- [4]. Han S-H, Lee M-A, An SS, Ahn S-W, Youn YC, Park K-Y (2014) Diagnostic value of Alzheimer's disease-related individual structural volume measurements using IBASPM. *J Clin Neurosci* 21, 2165–2169. [PubMed: 25150766]
- [5]. Burton EJ, Barber R, Mukaetova-Ladinska EB, Robson J, Perry RH, Jaros E, Kalaria RN, O'Brien JT (2009) Medial temporal lobe atrophy on MRI differentiates Alzheimer's disease from dementia with Lewy bodies and vascular cognitive impairment: A prospective study with pathological verification of diagnosis. *Brain* 132, 195–203. [PubMed: 19022858]
- [6]. Smith JC, Nielson KA, Woodard JL, Seidenberg M, Durgerian S, Hazlett KE, Figueroa CM, Kandah CC, Kay CD, Matthews MA, Rao SM (2014) Physical activity reduces hippocampal atrophy in elders at genetic risk for Alzheimer's disease. *Front Aging Neurosci* 6, 61. [PubMed: 24795624]
- [7]. Dickerson BC, Bakkour A, Salat DH, Feczko E, Pacheco J, Greve DN, Grodstein F, Wright CI, Blacker D, Rosas HD, Sperling RA, Atri A, Growdon JH, Hyman BT, Morris JC, Fischl B, Buckner RL (2009) The cortical signature of Alzheimer's disease: Regionally specific cortical thinning relates to symptom severity in very mild to mild AD dementia and is detectable in asymptomatic amyloid-positive individuals. *Cereb Cortex* 19, 497–510. [PubMed: 18632739]
- [8]. Wolk DA, Dickerson BC, Alzheimer's Disease Neuroimaging Initiative (2011) Fractionating verbal episodic memory in Alzheimer's disease. *Neuroimage* 54, 1530–1539. [PubMed: 20832485]
- [9]. Guo S, Lai C, Wu C, Cen G, Alzheimer's Disease Neuroimaging Initiative (2017) Conversion discriminative analysis on mild cognitive impairment using multiple cortical features from MR images. *Front Aging Neurosci* 9, 146. [PubMed: 28572766]
- [10]. Palta P, Schneider ALC, Biessels GJ, Touradji P, Hill-Briggs F (2014) Magnitude of cognitive dysfunction in adults with type 2 diabetes: A meta-analysis of six cognitive domains and the most frequently reported neuropsychological tests within domains. *J Int Neuropsychol Soc* 20, 278–291. [PubMed: 24555960]
- [11]. Moran C, Beare R, Phan TG, Bruce DG, Callisaya ML, Srikanth V, Alzheimer's Disease Neuroimaging Initiative (ADNI) (2015) Type 2 diabetes mellitus and biomarkers of neurodegeneration. *Neurology* 85, 1123–1130. [PubMed: 26333802]
- [12]. Schneider ALC, Selvin E, Sharrett AR, Griswold M, Coresh J, Jack CR, Knopman D, Mosley T, Gottesman RF (2017) Diabetes, prediabetes, and brain volumes and subclinical cerebrovascular disease on MRI: The Atherosclerosis Risk in Communities Neurocognitive Study (ARIC-NCS). *Diabetes Care* 40, 1514–1521. [PubMed: 28916531]
- [13]. Willette AA, Xu G, Johnson SC, Birdsill AC, +Jonaitis EM, Sager MA, Hermann BP, La Rue A, Asthana S, Bendlin BB (2013) Insulin resistance, brain atrophy, and cognitive performance in late middle-aged adults. *Diabetes Care* 36, 443–449. [PubMed: 23069842]
- [14]. (2017) 2017 Alzheimer's disease facts and figures. *Alzheimers Dement* 13, 325–373.
- [15]. Liu J, Liu T, Wang W, Ma L, Ma X, Shi S, Gong Q, Wang M (2017) Reduced gray matter volume in patients with type 2 diabetes mellitus. *Front Aging Neurosci* 9, 161. [PubMed: 28588480]
- [16]. Wu G, Lin L, Zhang Q, Wu J (2017) Brain gray matter changes in type 2 diabetes mellitus: A meta-analysis of whole-brain voxel-based morphometry study. *J Diabetes Complications* 31, 1698–1703. [PubMed: 29033311]
- [17]. Yeo BTT, Krienen FM, Sepulcre J, Sabuncu MR, Lashkari D, Hollinshead M, Roffman JL, Smoller JW, Zöllei L, Polimeni JR, Fischl B, Liu H, Buckner RL (2011) The organization of

- the human cerebral cortex estimated by intrinsic functional connectivity. *J Neurophysiol* 106, 1125–1165. [PubMed: 21653723]
- [18]. Seeley WW, Crawford RK, Zhou J, Miller BL, Greicius MD (2009) Neurodegenerative diseases target large-scale human brain networks. *Neuron* 62, 42–52. [PubMed: 19376066]
- [19]. Hoenig MC, Bischof GN, Seemiller J, Hammes J, Kukulja J, Onur ÖA, Jessen F, Fließbach K, Neumaier B, Fink GR, van Eimeren T, Drzezga A (2018) Networks of tau distribution in Alzheimer's disease. *Brain* 141, 568–581. [PubMed: 29315361]
- [20]. Grothe MJ, Teipel SJ, Alzheimer's Disease Neuroimaging Initiative (2016) Spatial patterns of atrophy, hypometabolism, and amyloid deposition in Alzheimer's disease correspond to dissociable functional brain networks. *Hum Brain Mapp* 37, 35–53. [PubMed: 26441321]
- [21]. McKhann GM, Knopman DS, Chertkow H, Hyman BT, Jack CR, Kawas CH, Klunk WE, Koroshetz WJ, Manly JJ, Mayeux R, Mohs RC, Morris JC, Rossor MN, Scheltens P, Carrillo MC, Thies B, Weintraub S, Phelps CH (2011) The diagnosis of dementia due to Alzheimer's disease: Recommendations from the National Institute on Aging–Alzheimer's Association workgroups on diagnostic guidelines for Alzheimer's disease. *Alzheimers Dement* 7, 263–269. [PubMed: 21514250]
- [22]. Beekly DL, Ramos EM, Lee WW, Deitrich WD, Jacka ME, Wu J, Hubbard JL, Koepsell TD, Morris JC, Kukull WA, NIA Alzheimer's Disease Centers (2007) The National Alzheimer's Coordinating Center (NACC) database: The Uniform Data Set. *Alzheimer Dis Assoc Disord* 21, 249–258. [PubMed: 17804958]
- [23]. Mohs RC, Rosen WG, Davis KL (1983) The Alzheimer's disease assessment scale: An instrument for assessing treatment efficacy. *Psychopharmacol Bull* 19, 448–450. [PubMed: 6635122]
- [24]. Rosenberg SJ, Ryan JJ, Prifitera A (1984) Rey Auditory-Verbal Learning Test performance of patients with and without memory impairment. *J Clin Psychol* 40, 785–787. [PubMed: 6746989]
- [25]. Calero MD, Navarro E (2004) Relationship between plasticity, mild cognitive impairment and cognitive decline. *Arch Clin Neuropsychol* 19, 653–660. [PubMed: 15271409]
- [26]. Crane PK, Carle A, Gibbons LE, Insel P, Mackin RS, Gross A, Jones RN, Mukherjee S, Curtis SM, Harvey D, Weiner M, Mungas D, Alzheimer's Disease Neuroimaging Initiative (2012) Development and assessment of a composite score for memory in the Alzheimer's Disease Neuroimaging Initiative (ADNI). *Brain Imaging Behav* 6, 502–516. [PubMed: 22782295]
- [27]. Gibbons LE, Carle AC, Mackin RS, Harvey D, Mukherjee S, Insel P, Curtis SM, Mungas D, Crane PK, Alzheimer's Disease Neuroimaging Initiative (2012) A composite score for executive functioning, validated in Alzheimer's Disease Neuroimaging Initiative (ADNI) participants with baseline mild cognitive impairment. *Brain Imaging Behav* 6, 517–527. [PubMed: 22644789]
- [28]. Dale A, Fischl B, Sereno MI (1999) Cortical surface-based analysis: I. Segmentation and surface reconstruction. *Neuroimage* 9, 179–194. [PubMed: 9931268]
- [29]. Dale AM, Sereno MI (1993) Improved localization of cortical activity by combining EEG and MEG with MRI cortical surface reconstruction: A linear approach. *J Cogn Neurosci* 5, 162–176. [PubMed: 23972151]
- [30]. Fischl B, Dale AM (2000) Measuring the thickness of the human cerebral cortex from magnetic resonance images. *Proc Natl Acad Sci U S A* 97, 11050–11055. [PubMed: 10984517]
- [31]. Fischl B, Liu A, Dale AM (2001) Automated manifold surgery: Constructing geometrically accurate and topologically correct models of the human cerebral cortex. *IEEE Med Imaging* 20, 70–80.
- [32]. Fischl B, Salat DH, Busa E, Albert M, Dieterich M, Haselgrove C, van der Kouwe A, Killiany R, Kennedy D, Klaveness S, Montillo A, Makris N, Rosen B, Dale AM (2002) Whole brain segmentation: Automated labeling of neuroanatomical structures in the human brain. *Neuron* 33, 341–355. [PubMed: 11832223]
- [33]. Fischl B, Salat DH, van der Kouwe AJW, Makris N, Ségonne F, Quinn BT, Dale AM (2004) Sequence-independent segmentation of magnetic resonance images. *Neuroimage* 23, S69–S84. [PubMed: 15501102]
- [34]. Fischl B, Sereno MI, Dale A (1999) Cortical surface-based analysis: II: Inflation, flattening, and a surface-based coordinate system. *Neuroimage* 9, 195–207. [PubMed: 9931269]

- [35]. Fischl B, Sereno MI, Tootell RBH, Dale AM (1999) High-resolution intersubject averaging and a coordinate system for the cortical surface. *Hum Brain Mapp* 8, 272–284. [PubMed: 10619420]
- [36]. Fischl B, van der Kouwe A, Destrieux C, Halgren E, Ségonne F, Salat DH, Busa E, Seidman LJ, Goldstein J, Kennedy D, Caviness V, Makris N, Rosen B, Dale AM (2004) Automatically parcellating the human cerebral cortex. *Cereb Cortex* 14, 11–22. [PubMed: 14654453]
- [37]. Han X, Jovicich J, Salat D, van der Kouwe A, Quinn B, Czanner S, Busa E, Pacheco J, Albert M, Killiany R, Maguire P, Rosas D, Makris N, Dale A, Dickerson B, Fischl B (2006) Reliability of MRI-derived measurements of human cerebral cortical thickness: The effects of field strength, scanner upgrade and manufacturer. *Neuroimage* 32, 180–194. [PubMed: 16651008]
- [38]. Jovicich J, Czanner S, Greve D, Haley E, Kouwe A van der, Gollub R, Kennedy D, Schmitt F, Brown G, MacFall J, Fischl B, Dale A (2006) Reliability in multi-site structural MRI studies: Effects of gradient non-linearity correction on phantom and human data. *Neuroimage* 30, 436–443. [PubMed: 16300968]
- [39]. Segonne F, Dale AM, Busa E, Glessner M, Salat D, Hahn HK, Fischl B (2004) A hybrid approach to the skull stripping problem in MRI. *Neuroimage* 22, 1060–1075. [PubMed: 15219578]
- [40]. Reuter M, Schmansky NJ, Rosas HD, Fischl B (2012) Within-subject template estimation for unbiased longitudinal image analysis. *Neuroimage* 61, 1402–1418. [PubMed: 22430496]
- [41]. Reuter M, Rosas HD, Fischl B (2010) Highly accurate inverse consistent registration: A robust approach. *Neuroimage* 53, 1181–1196. [PubMed: 20637289]
- [42]. Schwarz CG, Gunter JL, Wiste HJ, Przybelski SA, Weigand SD, Ward CP, Senjem ML, Vemuri P, Murray ME, Dickson DW, Parisi JE, Kantarci K, Weiner MW, Petersen RC, Jack CR, Alzheimer’s Disease Neuroimaging Initiative (2016) A large-scale comparison of cortical thickness and volume methods for measuring Alzheimer’s disease severity. *Neuroimage Clin* 11, 802–812. [PubMed: 28050342]
- [43]. Schmidt EL, Burge W, Visscher KM, Ross LA (2016) Cortical thickness in frontoparietal and cingulo-opercular networks predicts executive function performance in older adults. *Neuropsychology* 30, 322–331. [PubMed: 26460586]
- [44]. Braak H, Braak E (1991) Neuropathological stageing of Alzheimer-related changes. *Acta Neuropathol (Berl)* 82, 239–259. [PubMed: 1759558]
- [45]. Annese J, Schenker-Ahmed NM, Bartsch H, Maechler P, Sheh C, Thomas N, Kayano J, Ghatan A, Bresler N, Frosch MP, Klaming R, Corkin S (2014) Postmortem examination of patient H.M.’s brain based on histological sectioning and digital 3D reconstruction. *Nat Commun* 5, 3122. [PubMed: 24473151]
- [46]. Travis SG, Huang Y, Fujiwara E, Radomski A, Olsen F, Carter R, Seres P, Malykhin NV (2014) High field structural MRI reveals specific episodic memory correlates in the subfields of the hippocampus. *Neuropsychologia* 53, 233–245. [PubMed: 24296251]
- [47]. Sperling R, Chua E, Cocchiarella A, Rand-Giovannetti E, Poldrack R, Schacter DL, Albert M (2003) Putting names to faces: Successful encoding of associative memories activates the anterior hippocampal formation. *Neuroimage* 20, 1400–1410. [PubMed: 14568509]
- [48]. Takehara-Nishiuchi K (2014) Entorhinal cortex and consolidated memory. *Neurosci Res* 84, 27–33. [PubMed: 24642278]
- [49]. Ward AM, Schultz AP, Huijbers W, Van Dijk KRA, Hedden T, Sperling RA (2014) The parahippocampal gyrus links the default-mode cortical network with the medial temporal lobe memory system. *Hum Brain Mapp* 35, 1061–1073. [PubMed: 23404748]
- [50]. Yuan P, Raz N (2014) Prefrontal cortex and executive functions in healthy adults: A meta-analysis of structural neuroimaging studies. *Neurosci Biobehav Rev* 42, 180–192. [PubMed: 24568942]
- [51]. Dosenbach NUF, Fair DA, Miezin FM, Cohen AL, Wenger KK, Dosenbach RAT, Fox MD, Snyder AZ, Vincent JL, Raichle ME, Schlaggar BL, Petersen SE (2007) Distinct brain networks for adaptive and stable task control in humans. *Proc Natl Acad Sci U S A* 104, 11073–11078. [PubMed: 17576922]

- [52]. Fried PJ, Schilberg L, Brem A-K, Saxena S, Wong B, Cypess AM, Horton ES, Pascual-Leone A (2016) Humans with type-2 diabetes show abnormal long-term potentiation-like cortical plasticity associated with verbal learning deficits. *J Alzheimers Dis* 55, 89–100.
- [53]. Kilpatrick C, Murrie V, Cook M, Andrewes D, Desmond P, Hopper J (1997) Degree of left hippocampal atrophy correlates with severity of neuropsychological deficits. *Seizure* 6, 213–218. [PubMed: 9203250]
- [54]. Benjamini Y, Hochberg Y (1995) Controlling the false discovery rate: A practical and powerful approach to multiple testing. *J R Stat Soc Ser B Methodol* 57, 289–300.
- [55]. Smits LL, Tijms BM, Benedictus MR, Koedam ELGE, Koene T, Reuling IEW, Barkhof F, Scheltens P, Pijnenburg YAL, Wattjes MP, van der Flier WM (2014) Regional atrophy is associated with impairment in distinct cognitive domains in Alzheimer’s disease. *Alzheimers Dement* 10, S299–305. [PubMed: 24210526]
- [56]. Pascual B, Masdeu JC, Hollenbeck M, Makris N, Insausti R, Ding S-L, Dickerson BC (2015) Large-scale brain networks of the human left temporal pole: A functional connectivity MRI study. *Cereb Cortex* 25, 680–702. [PubMed: 24068551]
- [57]. Fan L, Wang J, Zhang Y, Han W, Yu C, Jiang T (2014) Connectivity-based parcellation of the human temporal pole using diffusion tensor imaging. *Cereb Cortex* 24, 3365–3378. [PubMed: 23926116]
- [58]. Allen EA, Erhardt EB, Damaraju E, Gruner W, Segall JM, Silva RF, Havlicek M, Rachakonda S, Fries J, Kalyanam R, Michael AM, Caprihan A, Turner JA, Eichele T, Adelsheim S, Bryan AD, Bustillo J, Clark VP, Feldstein Ewing SW, Filbey F, Ford CC, Hutchison K, Jung RE, Kiehl KA, Koditwakku P, Komesu YM, Mayer AR, Pearlson GD, Phillips JP, Sadek JR, Stevens M, Teuscher U, Thoma RJ, Calhoun VD (2011) A baseline for the multivariate comparison of resting-state networks. *Front Syst Neurosci* 5, 2. [PubMed: 21442040]
- [59]. Fox MD, Snyder AZ, Vincent JL, Corbetta M, Van Essen DC, Raichle ME (2005) The human brain is intrinsically organized into dynamic, anticorrelated functional networks. *Proc Natl Acad Sci U S A* 102, 9673–9678. [PubMed: 15976020]
- [60]. Chhatwal JP, Schultz AP, Johnson K, Benzinger TLS, Jack C, Ances BM, Sullivan CA, Salloway SP, Ringman JM, Koeppe RA, Marcus DS, Thompson P, Saykin AJ, Correia S, Schofield PR, Rowe CC, Fox NC, Brickman AM, Mayeux R, McDade E, Bateman R, Fagan AM, Goate AM, Xiong C, Buckles VD, Morris JC, Sperling RA (2013) Impaired default network functional connectivity in autosomal dominant Alzheimer disease. *Neurology* 81, 736–744. [PubMed: 23884042]
- [61]. Sperling RA, Laviolette PS, O’Keefe K, O’Brien J, Rentz DM, Pihlajamaki M, Marshall G, Hyman BT, Selkoe DJ, Hedden T, Buckner RL, Becker JA, Johnson KA (2009) Amyloid deposition is associated with impaired default network function in older persons without dementia. *Neuron* 63, 178–188. [PubMed: 19640477]
- [62]. Chen Y-C, Jiao Y, Cui Y, Shang S-A, Ding J, Feng Y, Song W, Ju S-H, Teng G-J (2014) Aberrant brain functional connectivity related to insulin resistance in type 2 diabetes: A resting-state fMRI study. *Diabetes Care* 37, 1689–1696. [PubMed: 24658392]
- [63]. Dennis EL, Thompson PM (2014) Functional brain connectivity using fMRI in aging and Alzheimer’s disease. *Neuropsychol Rev* 24, 49–62. [PubMed: 24562737]
- [64]. Krajcovicova L, Mikl M, Marecek R, Rektorova I (2014) Disturbed default mode network connectivity patterns in Alzheimer’s disease associated with visual processing. *J Alzheimers Dis* 41, 1229–1238. [PubMed: 24799341]
- [65]. Agosta F, Pievani M, Geroldi C, Copetti M, Frisoni GB, Filippi M (2012) Resting state fMRI in Alzheimer’s disease: Beyond the default mode network. *Neurobiol Aging* 33, 1564–1578. [PubMed: 21813210]
- [66]. Zarahn E, Rakitin B, Abela D, Flynn J, Stern Y (2007) Age-related changes in brain activation during a delayed item recognition task. *Neurobiol Aging* 28, 784–798. [PubMed: 16621168]
- [67]. Mucke L, Selkoe DJ (2012) Neurotoxicity of amyloid β -protein: Synaptic and network dysfunction. *Cold Spring Harb Perspect Med* 2, a006338. [PubMed: 22762015]

- [68]. Kim J, Yoon H, Basak J, Kim J (2014) Apolipoprotein E in synaptic plasticity and Alzheimer's disease: Potential cellular and molecular mechanisms. *Mol Cells* 37, 767–776. [PubMed: 25358504]
- [69]. Koudinov AR, Koudinova NV (2005) Cholesterol homeostasis failure as a unifying cause of synaptic degeneration. *J Neurol Sci* 229-230, 233–240. [PubMed: 15760645]
- [70]. Sanchez-Mejia RO, Newman JW, Toh S, Yu G-Q, Zhou Y, Halabisky B, Cissé M, Scearce-Levie K, Cheng IH, Gan L, Palop JJ, Bonventre JV, Mucke L (2008) Phospholipase A2 reduction ameliorates cognitive deficits in a mouse model of Alzheimer's disease. *Nat Neurosci* 11, 1311–1318. [PubMed: 18931664]
- [71]. Clark JK, Furgerson M, Crystal JD, Fehheimer M, Furukawa R, Wagner JJ (2015) Alterations in synaptic plasticity coincide with deficits in spatial working memory in presymptomatic 3xTg-AD mice. *Neurobiol Learn Mem* 125, 152–162. [PubMed: 26385257]
- [72]. Tamagnini F, Burattini C, Casoli T, Baliotti M, Fattoretti P, Aicardi G (2012) Early impairment of long-term depression in the perirhinal cortex of a mouse model of Alzheimer's disease. *Rejuvenation Res* 15, 231–234. [PubMed: 22533438]
- [73]. Ong W-Y, Tanaka K, Dawe GS, Ittner LM, Farooqui AA (2013) Slow excitotoxicity in Alzheimer's disease. *J Alzheimers Dis* 35, 643–668. [PubMed: 23481689]
- [74]. Wennberg AMV, Spira AP, Pettigrew C, Soldan A, Zipunnikov V, Rebok GW, Roses AD, Lutz MW, Miller MM, Thambisetty M, Albert MS (2016) Blood glucose levels and cortical thinning in cognitively normal, middle-aged adults. *J Neurol Sci* 365, 89–95. [PubMed: 27206882]
- [75]. Ott A, Stolk RP, van Harskamp F, Pols HA, Hofman A, Breteler MM (1999) Diabetes mellitus and the risk of dementia: The Rotterdam Study. *Neurology* 53, 1937–1942. [PubMed: 10599761]
- [76]. Talbot K, Wang H-Y, Kazi H, Han L-Y, Bakshi KP, Stucky A, Fuino RL, Kawaguchi KR, Samoyedny AJ, Wilson RS, Arvanitakis Z, Schneider JA, Wolf BA, Bennett DA, Trojanowski JQ, Arnold SE (2012) Demonstrated brain insulin resistance in Alzheimer's disease patients is associated with IGF-1 resistance, IRS-1 dysregulation, and cognitive decline. *J Clin Invest* 122, 1316–1338. [PubMed: 22476197]
- [77]. Young AL, Oxtoby NP, Daga P, Cash DM, Fox NC, Ourselin S, Schott JM, Alexander DC, Alzheimer's Disease Neuroimaging Initiative (2014) A data-driven model of biomarker changes in sporadic Alzheimer's disease. *Brain* 137, 2564–2577. [PubMed: 25012224]
- [78]. Chen Z, Sun J, Yang Y, Lou X, Wang Y, Wang Y, Ma L (2015) Cortical thinning in type 2 diabetes mellitus and recovering effects of insulin therapy. *J Clin Neurosci* 22, 275–279. [PubMed: 25439756]
- [79]. Nardone R, Tezzon F, Höller Y, Golaszewski S, Trinkka E, Brigo F (2014) Transcranial magnetic stimulation (TMS)/repetitive TMS in mild cognitive impairment and Alzheimer's disease. *Acta Neurol Scand* 129, 351–366. [PubMed: 24506061]
- [80]. Gonsalvez I, Baror R, Fried P, Santarnecchi E, Pascual-Leone A (2017) Therapeutic noninvasive brain stimulation in Alzheimer's disease. *Curr Alzheimer Res* 14, 362–376. [PubMed: 27697061]

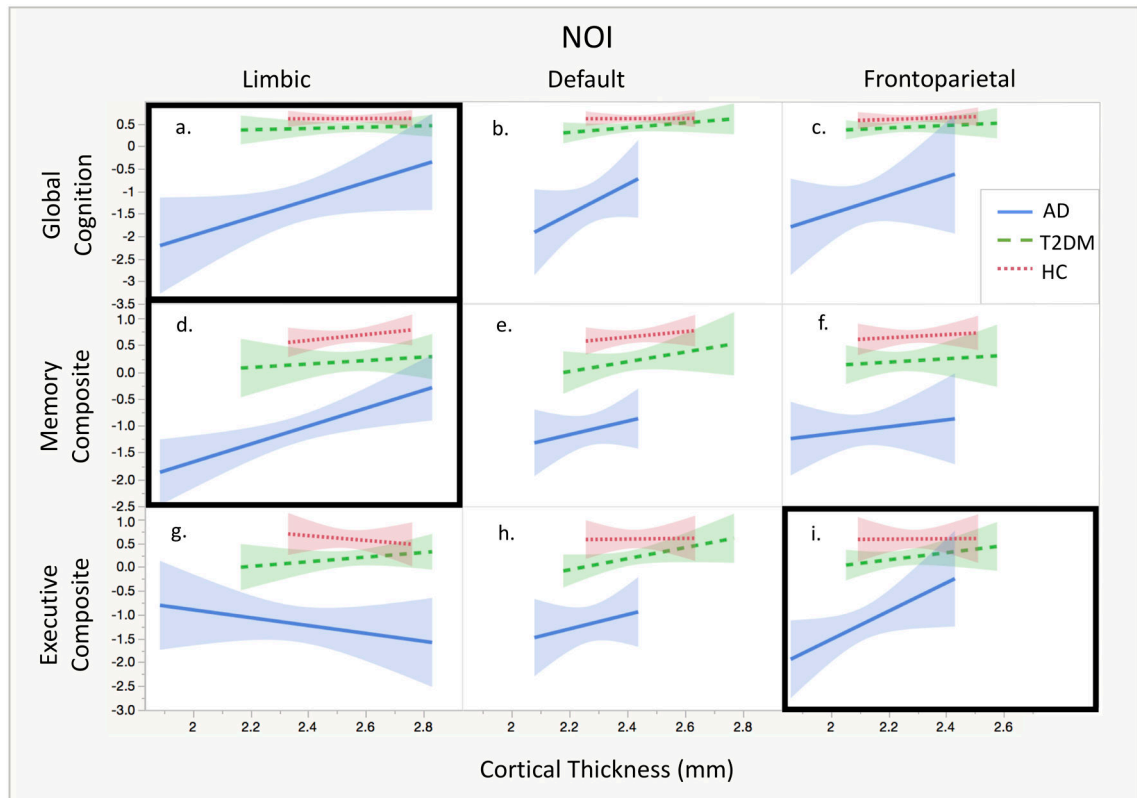


Fig. 1.

NOI thickness and cognitive composite scores. Within each NOI, linear regression between cortical thickness and cognitive composite scores are shown. Models which were significant based on uncorrected p-values are marked with a black box. (a) There is a significant relationship between cortical thickness in the limbic NOI and Global Cognition, (d) between cortical thickness in the limbic NOI and Memory Composite, and (i) between cortical thickness in the frontoparietal NOI and Executive Composite.

Table 1

Baseline characteristics

	Significance Tests			
	df	F ratio	p-value	Tukey's HSD
Number (#)	27	28	22	
Female # (%)	12 (44%)	13 (46%)	13 (59%)	N = 77, df = 2, 2-tailed $p = 0.578$; Fisher's Exact Test
Age (y)	61.7 ± 1.6	66.3 ± 1.5	69.6 ± 1.7	2,74 5.96 0.004 HC<AD
MMSE (#/30)	29.4 ± 0.3	29.0 ± 0.3	21.8 ± 0.3	2,74 196.90 <0.001 AD<HC, T2DM
GDS (#/15)	0.5 ± 0.3	1.2 ± 0.3	2.4 ± 0.4	2,74 7.31 0.001 HC<AD
Education (y)	15.8 ± 0.6	15.5 ± 0.5	16.6 ± 0.6	2,74 0.86 0.429
Premorbid IQ (W-TAR)	113.6 ± 2.4	112.2 ± 2.4	108.2 ± 2.7	2,74 1.19 0.311
Network ROI thicknesses (mm)				
Limbic NOI Thickness	2.5 ± 0.03	2.5 ± 0.03	2.4 ± 0.03	2,74 11.70 <0.001 AD<HC, T2DM
Default NOI Thickness	2.4 ± 0.02	2.4 ± 0.02	2.3 ± 0.02	2,74 15.60 <0.001 AD<HC, T2DM
Frontoparietal NOI Thickness	2.3 ± 0.02	2.2 ± 0.02	2.1 ± 0.02	2,74 17.90 <0.001 AD<HC, T2DM
Hippocampal Volume (z-scores)				
RH hippocampal volume/eTIV	0.4 ± 0.2	0.2 ± 0.2	-0.8 ± 0.2	2,74 15.50 <0.001 AD<HC, T2DM
LH hippocampal volume/eTIV	0.4 ± 0.2	0.3 ± 0.2	-0.9 ± 0.2	2,74 20.00 <0.001 AD<HC, T2DM
Global Cognition (z-scores)				
ADAS-Cog Total (inverse)	0.6 ± 0.1	0.4 ± 0.1	-1.2 ± 0.1	2,74 75.30 <0.001 AD<HC, T2DM
Memory Composite (z-scores)				
RAVLT Immediate Recall	0.7 ± 0.1	0.2 ± 0.1	-1.1 ± 0.1	2,74 85.11 <0.001 AD<T2DM<HC
RAVLT Delayed Recall	0.6 ± 0.1	0.3 ± 0.1	-1.1 ± 0.1	2,74 65.10 <0.001 AD<T2DM<HC
RAVLT Delayed Recognition	0.6 ± 0.1	0.2 ± 0.1	-1.0 ± 0.2	2,74 43.00 <0.001 AD<HC, T2DM
LMS Immediate Recall	0.8 ± 0.1	0.05 ± 0.1	-1.0 ± 0.2	2,74 30.30 <0.001 AD<HC, T2DM
LMS Delayed Recall	0.7 ± 0.1	0.1 ± 0.1	-1.0 ± 0.2	2,74 36.08 <0.001 AD<T2DM<HC
ADAS-Cog Immediate Recall (inverse)	0.8 ± 0.1	0.2 ± 0.1	-1.2 ± 0.1	2,74 33.10 <0.001 AD<T2DM<HC
ADAS-Cog Delayed Recognition (inverse)	0.4 ± 0.2	0.3 ± 0.2	-1.0 ± 0.2	2,74 66.60 <0.001 AD<T2DM<HC
Executive Composite (z-scores)				
DSB Length	0.6 ± 0.1	0.2 ± 0.1	-1.2 ± 0.1	2,74 19.80 <0.001 AD<HC, T2DM
DSST	0.5 ± 0.2	0.05 ± 0.2	-0.7 ± 0.2	2,74 60.20 <0.001 AD<T2DM<HC
	0.7 ± 0.1	0.2 ± 0.1	-1.2 ± 0.1	2,74 12.10 <0.001 AD<HC, T2DM
				2,73 59.50 <0.001 AD<T2DM<HC

	Significance Tests			AD	T2DM	HC
	F ratio	p-value	Tukey's HSD			
TMT B-A (inverse)	50.00	<0.001	AD<HC, T2DM	-1.4 ± 0.2	0.3 ± 0.1	0.5 ± 0.1
	df					
	2,67					

Gender proportions are shown using Fisher's exact test. All other results are presented as Mean ± Std error generated from ANOVA. Significant values with $p < 0.05$ are shown in bold, and are further characterized using Tukey's HSD to compare means between all three groups.